Manipulating the spin texture in a spin-orbit superlattice by terahertz radiation

D. V. Khomitsky*
Department of Physics, University of Nizhny Novgorod, 23 Gagarin Avenue, 603950 Nizhny Novgorod, Russia
(Received 20 August 2007; revised manuscript received 16 February 2008; published 31 March 2008)

The spin texture in a gate-controlled one-dimensional superlattice with Rashba spin-orbit coupling is studied in the presence of external terahertz radiation causing the superlattice miniband transitions. It is shown that the local distribution of the excited spin density can be modified by varying the Fermi level of the electron gas and by changing the radiation intensity and polarization, allowing the controlled coupling of spins and photons.

DOI: 10.1103/PhysRevB.77.113313 PACS number(s): 72.25.Fe, 73.21.Cd

I. INTRODUCTION

The control of the spin degrees of freedom is one of the primary goals of the rapidly developing field of condensed matter physics known as spintronics.[1,2] In addition to the methods involving the magnetic field which effectively governs the spins, the application of nonmagnetic spin systems can be considered by taking into account the spin-orbit (SO) interaction. In most widely considered two-dimensional semiconductor heterostructures, the SO interaction is usually dominated by the Rashba coupling[3] coming from the structure inversion asymmetry of the confining potential and effective mass difference. The value of the Rashba coupling strength can be tuned by the external gate voltage[4] and it reaches the value of 2×10^{-11} eV m in InAs-based structures.[5] One of the important issues in spintronics is the interaction between spins and photons, which is promising for further applications in novel electronic and optical devices. The studies of the optical properties of SO semiconductor structures have formed a fast growing field of studies during the past decade. Some of the research topics included the photogalvanic,[6,7,9–12] spin-galvanic,[8,9] and spin-photovoltaic[13] effects as well as optical spin orientation[14] and pure spin current generation.[15,16] The effects of terahertz radiation onto spin-split states in semiconductors were also the subject of investigation.[17,18] Another important property of nonuniform spin distributions such as spin coherence standing waves was discussed by Pershin,[19] who found an increase in the spin relaxation time in such structures, making them promising for spintronics applications. One of the possible ways to create a nonuniform spin distribution in a heterostructure is to apply a metal-gated superlattice with electric potential of tunable amplitude to the two-dimensional electron gas (2DEG) with spin-orbit coupling. The quantum states and spin polarization in this system with standing spin waves were studied previously,[20] and the problem of scattering on such a structure has been considered.[21]

In this Brief Report, we study the problem of the excited spin density creation in a one-dimensional InAs-based superlattice with Rashba spin-orbit coupling by applying an external terahertz radiation. The direction of photon propagation is chosen to be perpendicular to the 2DEG plane where both linear and circular polarizations are considered. It is shown that the excited spin texture is sensitive to the position of the Fermi level of the 2DEG and to the radiation intensity. The former can be tuned by the gate voltage, thus providing a possible way to couple local excited distribution of spins and photons in 2DEG with SO interaction. The obtained results have a qualitative character and are not restricted to one specific type of semiconductor heterostructure, superlattice period, amplitude of periodic potential, Fermi level position, etc. Another important issue is the spin relaxation which tends to transform the excited spin distribution back to equilibrium. The terahertz scale of excitation frequencies is at least an order of magnitude larger than the spin relaxation rates in InAs semiconductor heterostructures which can be estimated as $1/\tau_s$, where the spin lifetime τ_s reaches values from 60 ps (Ref. 22) to 600 ps (Ref. 23) and the spin relaxation time is further increased in nonhomogeneous spin textures.[19] Thus, one can expect that the effects discussed in this Brief Report can be experimentally observed.

This Brief Report is organized as follows. In Sec. II, we briefly describe quantum states in a SO superlattice and in Sec. III, we calculate the spatial distribution of the excited spin density in a superlattice cell under terahertz radiation with different positions of the Fermi level, radiation intensities, and polarizations. The conclusions are given in Sec. IV.

II. QUANTUM STATES IN SPIN-ORBIT SUPERLATTICE

We start with the brief description of the quantum states of 2DEG with Rashba SO coupling and one-dimensional (1D) periodic superlattice potential in the absence of external electromagnetic field.[20] The Hamiltonian is the sum of the 2DEG kinetic energy operator in a single size quantization band with effective mass m, the Rashba SO term with strength α, and the periodic electrostatic potential of the 1D superlattice,

$$\hat{H} = \frac{\hat{p}^2}{2m} + \alpha(\hat{\sigma}_x\hat{p}_y - \hat{\sigma}_y\hat{p}_x) + V(x), \tag{1}$$

where $\hbar=1$ and the periodic potential is chosen in the simplest form $V(x)=V_0\cos 2\pi x/a$, where a is the superlattice period and the amplitude V_0 is controlled by the gate voltage. The eigenstates of Hamiltonian (1) are two-component Bloch spinors with eigenvalues labeled by the quasimomentum k_x in a one-dimensional Brillouin zone $-\pi/a\leqslant k_x\leqslant\pi/a$, the momentum component k_y, and the miniband index m:

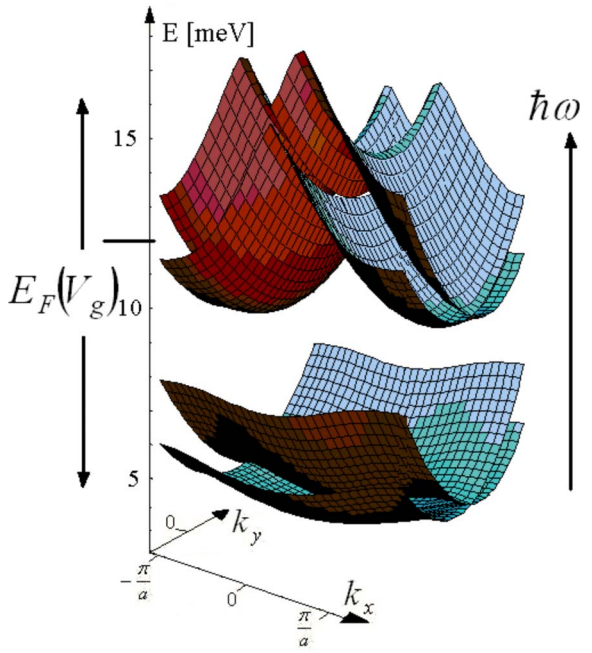

FIG. 1. (Color online) Energy spectrum of the four lowest minibands in the InAs 1D superlattice with Rashba constant $\alpha=2\times10^{-11}$ eV m, the electron effective mass $m=0.036m_0$, the superlattice period $a=60$ nm, and the amplitude $V_0=10$ meV. The Fermi level position $E_F(V_g)$ and the photon energy $\hbar\omega=10$ meV corresponding to $\omega/2\pi=2.43$ THz are shown schematically.

$$\psi_{m\mathbf{k}} = \sum_{\lambda n} a_{\lambda n}^{m}(\mathbf{k}) \frac{e^{i\mathbf{k}_n\mathbf{r}}}{\sqrt{2}} \begin{pmatrix} 1 \\ \lambda e^{i\theta_n} \end{pmatrix}, \quad \lambda = \pm 1. \tag{2}$$

Here, $\mathbf{k}_n=\mathbf{k}+n\mathbf{b}=(k_x+\frac{2\pi}{a}n,k_y)$ and $\theta_n=\arg[k_y-ik_{nx}]$. The energy spectrum of Hamiltonian (1) consists of pairs of spin-split minibands determined by the SO strength α separated by the gaps of the order of V_0. An example of the energy spectrum is shown in Fig. 1 for the four lowest minibands in the InAs 1D superlattice with Rashba constant $\alpha=2\times10^{-11}$ eV m, the electron effective mass $m=0.036m_0$, the superlattice period $a=60$ nm, and the amplitude of the periodic potential $V_0=10$ meV. It should be mentioned that the spectrum in Fig. 1 is limited to the first Brillouin zone of the superlattice in the k_x direction, while the cutoff in the k_y direction is only shown to keep the limits along k_x and k_y comparable. The Fermi level position $E_F(V_g)$ can be varied by tuning the gate voltage which controls the concentration of the 2D electrons. This feature is shown in Fig. 1 schematically by the arrows near $E_F(V_g)$ as well as the photon energy $\hbar\omega=10$ meV corresponding to $\omega/2\pi=2.43$ THz.

III. SPIN TEXTURE MANIPULATION

The Rashba SO coupling as well as the periodic superlattice potential cannot produce the net polarization of 2DEG. Moreover, the two-component eigenvectors of the Rashba Hamiltonian describe the homogeneous local spin density $\sigma_i=\psi^\dagger\hat{\sigma}_i\psi$, where $i=x,y,z$. In the presence of an additional superlattice potential, however, the local spin density for a given state (k_x,k_y) can be inhomogeneous,[20] as in the spin coherence standing wave,[19] which gives an idea on how to obtain a nonuniform spin density distribution under an external radiation which, in transitions, involves the states with different (k_x,k_y) with a varying impact depending on the matrix elements. In this section, we subject the 2DEG with Hamiltonian (1) to the electromagnetic radiation propagating along the z axis perpendicular to the 2DEG plane with the electric field of the radiation $\mathbf{E}(t)=\mathbf{e}E_\omega \exp^{-i\omega t}+\text{c.c.}$, with amplitude E_ω, frequency ω, and polarization $\mathbf{e}=(e_x,e_y)$. When the electromagnetic radiation is applied, the excited spin density rate S_i at a given point in a real space can be found in the following way:[15]

$$S_i = \frac{\pi e^2 E_\omega^2}{\omega^2} \int d^2k \sum_{jl} \xi_i^{jl}(\mathbf{k}) \bar{e}_j e_l, \tag{3}$$

where

$$\xi_i^{jl}(\mathbf{k}) = \sum_{c,m,m'} (\psi_{m'}^\dagger \hat{\sigma}_i \psi_m) \bar{v}_{m'c}^{j} v_{mc}^{l} \tag{4}$$

$$\times \{\delta[\omega_{mc}(\mathbf{k})-\omega]+\delta[\omega_{m'c}(\mathbf{k})-\omega]\}. \tag{5}$$

Since the structure is completely homogeneous in the y direction, the S_y component vanishes. The other components S_x and S_z of the excited nonequilibrium spin density can be nonzero at a given point in a superlattice even for the linear x-polarized radiation. The coexistence of the axial vector components (S_x,S_z) in the left side of Eq. (3), together with the polar vector component e_x in the right side, is in agreement with the principles of magnetic crystal class analysis.[24] There is a mirror plane of reflection σ_y in our system which changes y to $-y$, and thus changes the sign of the magnetic moment, leaving the e_x component of the polarization unchanged. The element of the magnetic crystal class, however, is applied only as a combination $\sigma_y R$, where R is the time reversal operator,[24] which again changes the direction of the magnetic moment but does not change the polarization component e_x. As a result, the combination $\sigma_y R$ leaves both spin projections $S_{x,z}$ and the polarization component e_x invariant. Another restriction is the absence of total magnetic moment of the sample which means that both S_x and S_z must satisfy the requirement of zero net polarization:

$$\int_0^a S_x(x)dx = \int_0^a S_z(x)dx = 0. \tag{6}$$

The spin density distribution in the superlattice cell is found for three different polarizations: linear along the x axis, linear along the y axis, and circular in the xy plane of 2DEG. The Fermi level in Fig. 1 varies from 4 to 20 meV, counted from the bottom of the topmost partially filled electron size quantization band. According to the spectrum in Fig. 1, this variation gradually fills all four minibands shown there. The excitation energy is chosen to be $\hbar\omega=10$ meV, which corresponds to $\omega/2\pi=2.43$ THz and provides effective transitions between the occupied and vacant minibands, as can be seen in Fig. 1.

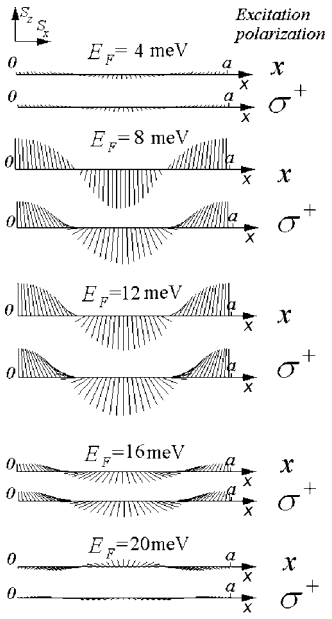

FIG. 2. Excited spin density distribution $[S_x(x), S_z(x)]$ along the 1D superlattice elementary cell created under x- and σ^+-polarized terahertz excitations with the frequency $\omega/2\pi$=2.43 THz and with the intensity I=0.3 W/cm^2.

First, let us consider the cases of the excitation linearly polarized along the x axis and the σ^+-circular polarized one. The excited nonequilibrium spin density (3) is shown in Fig. 2 as a 2D vector field $[S_x(x), S_z(x)]$. Its magnitude is proportional to the radiation intensity, which is 0.3 W/cm^2 for the present case, and the texture shape is varied with respect to the Fermi energy. The magnitude of the arrow length in Fig. 2, i.e., the maximum excited spin density, can be obtained from the value of the excited charge density n_{ex}. Taking the data from the experiments with optical excitation[17] where the volume concentration of the excited carriers reached 10^{16} cm^{-3}, one can estimate the excited surface concentration n_{ex} to be of the order of $10^{10}-10^{11}$ cm^{-2}. One can see in Fig. 2 that the spin textures are similar for x and σ^+ radiations, as well as for σ^- (not shown). The explanation is that all these polarizations contain the x component of transition matrix elements which causes the most effective transitions in the x-oriented superlattice. The transformation of spin density distribution with the Fermi level position in Fig. 2 is produced by gradual filling of the minibands. The small amplitudes of spin density (at E_F=4 meV in Fig. 2) correspond to the small filling factor (see Fig. 1). By increasing the Fermi energy, the complete filling of two lowest subbands (at E_F=8 meV and E_F=12 meV in Fig. 2) is reached and, finally, the excited spin density magnitude decreases again with complete filling of all four nearest minibands in Fig. 1 (at E_F=16 meV and E_F=20 meV in Fig. 2). It can be seen in Fig. 2 that the excited spin density texture has the primary spatial wavelength close to the superlattice period a. This feature can be explained by the structure of the matrix element of the transitions which reaches maximum amplitude at $k_x=\pm\pi/a$, leading to the effective creation of spin texture (3) with the specific primary wavelength equal to a. Since the Fermi level position can be varied in experiments by tuning the gate voltage which controls the concentration of 2DEG, our model predicts a possible and realistic mechanism for optical creation of various spin textures.

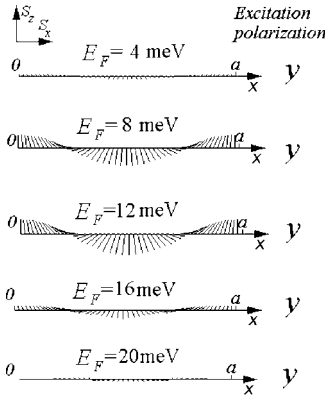

FIG. 3. Excited spin density distribution $[S_x(x), S_z(x)]$ along the 1D superlattice elementary cell created under y-polarized terahertz excitation with the same parameters as in Fig. 2 but at higher intensity I=0.9 W/cm^2.

Another type of the considered polarization is the radiation polarized along the y axis. The structure is homogeneous in this direction and the only reason for the transition probabilities to be nonzero is the nonparabolic character of the energy spectrum as a function of k_y due to the interplay between SO and superlattice potentials. However, this interplay is reduced with increasing k_y, and thus one can expect the probabilities to be smaller for the y-polarized radiation than for the x-polarized one, making the creation of the excited spin texture comparable to the one in Fig. 2 possible at higher intensities. This suggestion is confirmed by the spin textures in Fig. 3, where the same spin textures as in Fig. 2 are created at the intensity of 0.9 W/cm^2, which is three times greater than that for the x- and σ-polarized light. Nevertheless, all of the intensities considered in this Brief Report are within the range of 0.5–1 W/cm^2, which is accessible in modern experimental setups.[9,10,12,16,17]

Further investigations of gated 2DEG with SO interaction would require the studies of the spin current conventionally described by the operator $\hat{j}^s_{ij}=\hbar\{\hat{v}_i,\hat{\sigma}_j\}/4$, where $\hbar\hat{v}_i=\partial\hat{H}/\partial k_i$. The excited spin current distribution can be analyzed under the same approach as the spin density, and the spin separation distance can be calculated.[15] The investigations of spin current in our system deserve a separate detailed discussion and will be performed in a forthcoming paper.

IV. CONCLUSIONS

We have studied the excited spin texture distribution in 2DEG with Rashba spin-orbit interaction subject to 1D tunable superlattice potential and illuminated by terahertz radiation with different polarizations and intensities. It was found that in the absence of the net polarization, the local excited spin texture can be effectively manipulated by varying the

Fermi level position in 2DEG as well as the intensity and polarization of the radiation at fixed terahertz frequency. The effect of excited spin texture creation discussed in this Brief Report has a qualitative character and should be observable in a wide class of two-dimensional heterostructures where the spin-orbit coupling energy is more pronounced than the temperature broadening or the smearing caused by edges, defects, or impurities.

ACKNOWLEDGMENTS

The author thanks V. Ya. Demikhovskii and A. A. Perov for many helpful discussions. The work was supported by the RNP Program of the Ministry of Education and Science RF, by the RFBR, by the CRDF, and by the Foundation "Dynasty" (ICFPM).

*khomitsky@phys.unn.ru

[1] *Semiconductor Spintronics and Quantum Computation*, edited by D. D. Awschalom, D. Loss, and N. Samarth (Springer, Berlin, 2002).
[2] I. Zutić, J. Fabian, and S. Das Sarma, Rev. Mod. Phys. **76**, 323 (2004).
[3] E. I. Rashba, Fiz. Tverd. Tela (Leningrad) **2**, 1224 (1960) [Sov. Phys. Solid State **2**, 1109 (1960)]; Y. A. Bychkov and E. I. Rashba, J. Phys. C **17**, 6039 (1984).
[4] J. B. Miller, D. M. Zumbühl, C. M. Marcus, Y. B. Lyanda-Geller, D. Goldhaber-Gordon, K. Campman, and A. C. Gossard, Phys. Rev. Lett. **90**, 076807 (2003).
[5] D. Grundler, Phys. Rev. Lett. **84**, 6074 (2000).
[6] L. E. Golub, Phys. Rev. B **67**, 235320 (2003).
[7] S. D. Ganichev, V. V. Bel'kov, Petra Schneider, E. L. Ivchenko, S. A. Tarasenko, W. Wegscheider, D. Weiss, D. Schuh, E. V. Beregulin, and W. Prettl, Phys. Rev. B **68**, 035319 (2003).
[8] S. D. Ganichev, Petra Schneider, V. V. Bel'kov, E. L. Ivchenko, S. A. Tarasenko, W. Wegscheider, D. Weiss, D. Schuh, B. N. Murdin, P. J. Phillips, C. R. Pidgeon, D. G. Clarke, M. Merrick, P. Murzyn, E. V. Beregulin, and W. Prettl, Phys. Rev. B **68**, 081302(R) (2003).
[9] S. Giglberger, L. E. Golub, V. V. Bel'kov, S. N. Danilov, D. Schuh, C. Gerl, F. Rohlfing, J. Stahl, W. Wegscheider, D. Weiss, W. Prettl, and S. D. Ganichev, Phys. Rev. B **75**, 035327 (2007).
[10] C. L. Yang, H. T. He, Lu Ding, L. J. Cui, Y. P. Zeng, J. N. Wang, and W. K. Ge, Phys. Rev. Lett. **96**, 186605 (2006).
[11] Bin Zhou and Shun-Quing Shen, Phys. Rev. B **75**, 045339 (2007).
[12] K. S. Cho, C.-T. Liang, Y. F. Chen, Y. Q. Tang, and B. Shen, Phys. Rev. B **75**, 085327 (2007).
[13] Arkady Fedorov, Yuriy V. Pershin, and Carlo Piermarocchi, Phys. Rev. B **72**, 245327 (2005).
[14] S. A. Tarasenko, Phys. Rev. B **73**, 115317 (2006).
[15] R. D. R. Bhat, F. Nastos, Ali Najmaie, and J. E. Sipe, Phys. Rev. Lett. **94**, 096603 (2005).
[16] Hui Zhao, Xinyu Pan, Arthur L. Smirl, R. D. R. Bhat, Ali Najmaie, J. E. Sipe, and H. M. van Driel, Phys. Rev. B **72**, 201302(R) (2005).
[17] J. T. Olesberg, Wayne H. Lau, Michael E. Flatté, C. Yu, E. Altunkaya, E. M. Shaw, T. C. Hasenberg, and Thomas F. Boggess, Phys. Rev. B **64**, 201301(R) (2001).
[18] Jacob B. Khurgin, Phys. Rev. B **73**, 033317 (2006).
[19] Yuriy V. Pershin, Phys. Rev. B **71**, 155317 (2005).
[20] V. Ya. Demikhovskii and D. V. Khomitsky, JETP Lett. **83**, 340 (2006) [Pis'ma Zh. Eksp. Teor. Fiz. **83**, 399 (2006)].
[21] D. V. Khomitsky, Phys. Rev. B **76**, 033404 (2007).
[22] B. N. Murdin, K. Litvinenko, J. Allam, C. R. Pidgeon, M. Bird, K. Morrison, T. Zhang, S. K. Clowes, W. R. Branford, J. Harris, and L. F. Cohen, Phys. Rev. B **72**, 085346 (2005).
[23] K. C. Hall, K. Gündoğdu, E. Altunkaya, W. H. Lau, Michael E. Flatté, Thomas F. Boggess, J. J. Zinck, W. B. Barvosa-Carter, and S. L. Skeith, Phys. Rev. B **68**, 115311 (2003).
[24] L. D. Landau and E. M. Lifshitz, *Electrodynamics of Continuous Media* (Pergamon, New York, 1984).